

All-optically Controlled Microwave Analog Phase Shifter with Insertion Losses Balancing

J. Li, *Member, IAENG*

Abstract—An all-optically driven microwave phase shifter is designed and experimentally demonstrated for 1–10 GHz. The proposed optical addressing is realised in nematic liquid crystals (NLC) mixed with novel mesogenic azobenzene (azo) dyes, allowing a dielectric constant variation from a surface anchoring nematic state to a photo-induced isotropic state when exposed to a laser beam with a wavelength of 465 nm. The phase shifter device is implemented in a compact meandered inverted microstrip with impedance matched by a novel light-intensity-dependent method for insertion loss balancing between tuning states. Prototyped by photolithography, the device is assembled with an azo NLC mixture of GT3-24002 and CPND-7 (10wt%). Measurements report a continuously tunable differential phase shift of 0–184° at 10 GHz with a maximum insertion loss of –3.53 dB and negligible insertion loss variations (up to 9%) between phase-shifting states, which eliminates complex phase-biasing networks and amplitude-compensating circuits for the standalone high-resolution phased array beamforming application with reduced distortions.

Index Terms—Beam steering, delay lines, liquid crystals, mesogenic azo dye, microwave devices, phase shifters

I. INTRODUCTION

MICROWAVE and millimetre-wave beam steering desire ultra-fine scanning resolutions for applications in radio astronomical instrumentation, high-resolution imaging, and uninterrupted communication between antennas in a constantly varying environment [1]. The key technology to realise this is through precise delays of the modulated microwave signal at each antenna array element [2]. The current status of phased array exhibits limited steering resolutions, due mainly to the digital nature of switches-based phase shifters [1]. Ongoing innovations in tunable dielectrics such as nematic liquid crystals (NLC) [3]–[6] have enabled continuously variable delay lines for analog beamforming [7]–[9], but practical resolution performance is significantly degraded by noises due to the complex biasing circuits and amplitude compensation networks. Current status [5] in the driving approach for NLC’s molecular reorientations are predominately through electric or magnetic field biasing. These methods struggle to obviate the need for bias tees (to

discriminate microwave signal and low-frequency voltage bias) in electrical tuning, and power-consuming bulky magnets embedded in magnetic tuning. Moreover, existing NLC-based phase shifters [7][10]–[13] have yet to address insertion losses unbalancing between different phase-shifting states, resulting in undesirable distortions in beam steering, and hence the need for additional amplitude compensating networks [1][2]. Arguably, the biasing and compensation networks with high complexity significantly limit the NLC-based phase shifters for integrated into a larger phased array beamforming system.

In this letter, a novel optically driven low-loss method is demonstrated free of the biasing circuits and amplitude compensation networks. The proposed solution is based on modulating a laser beam’s intensity illuminating a highly anisotropic NLC (GT3-24002) doped with 10 wt% mesogenic azobenzene (azo) dye (CPND-7) at room temperature. The photoexcited trans-to-cis photoisomerization [14] of the azobenzene results in a nematic-to-isotropic phase transition of the LC, and hence a variation in the effective dielectric constant when interacting with a microwave signal. Based on this mechanism, we apply the mesogenic azo LC mixture as a tunable dielectric layer for an inverted microstrip line structure to realise an optically controlled phase shifter at 1-10 GHz. The achievable differential phase shift ($\Delta\Phi_{21}$) for a microwave signal of frequency (f) is governed by (1), where L is the effective line length within the laser beam spot of intensity I , c_0 is the free-space light speed, $\epsilon_{eff}(I)$ and $\epsilon_{eff}(I=0)$ denote the effective permittivity of the structure illuminated by the laser beam intensity of I , and beam turned-off, respectively.

$$\Delta\Phi_{21} = \frac{2\pi f L}{c_0} (\sqrt{\epsilon_{eff}(I)} - \sqrt{\epsilon_{eff}(I=0)}) \quad (1)$$

By manipulation of the coherent light source only, our all-optical method eliminates the circuit complexity due to electric or magnetic biasing networks when integrating multiple delay lines into a beamforming module. As distinct from traditional NLC photoalignment methods [15] based on spin-coating non-mesogenic azo dye films (e.g. Methyl Red) exposed to UV light, this work employs a novel mesogenic azo dye (CPND-7) with a shifted absorption peak into the visible spectrum. More fundamentally, the mesogenic nature enables a higher concentration (10 wt%) of the azo dye to be mixed with the NLC, hence a faster and stronger tunability. While mesogenic azo LC for fast reversible optical switching has been investigated for visible wavelengths [16], the distinct properties have yet to be explored for microwave and millimetre-wave

Manuscript received April 20, 2020; revised July 6, 2020. This work was supported in part by the Centre for Photonic Devices and Sensors, University of Cambridge.

J. Li is with Department of Electrical and Electronic Engineering, Imperial College London, London SW7 2AZ, United Kingdom, and Centre for Electronics Frontiers, University of Southampton, Southampton SO17 1BJ, United Kingdom (corresponding author e-mail: jinfeng.li@imperial.ac.uk).

tunable components. To build a bridge between the mesogenic azo LC optical technology and reconfigurable microwave components, this work, to the best of the author's knowledge, demonstrates the first all-optically driven 0–180° analog phase shifter at 10 GHz. Additionally, a novel impedance-matching method is incorporated for insertion losses balancing between different phase-shifting states, hence obviates the need for amplifiers and amplitude compensating networks.

II. PHASE SHIFTER DEVICE DESIGN

The proposed optically driven phase shifter is implemented in an inverted microstrip (see Fig. 1), with a core line realised in an optically transparent conductor coated on a transparent substrate. A meandering section is continuously confined within the beam diameter of 3 cm where photoexcitation of the azo LC is effective. Indium-tin oxide (ITO) coated glass and duralumin grounding plates are used for the first prototype. The tunable delay lines are designed not just with a low insertion loss, but also a comparatively constant loss level within the phase tuning range at each frequency. This is aimed for minimising beam distortions during steering, as signals combining and nulls forming (at undesirable directions) are significantly affected by the signal amplitude at each channel [2]. Due to LC's molecular shape anisotropy, the dielectric properties (permittivity, dissipation factor) and characteristic impedance both vary with the light intensity. The delay line geometry design is strategically impedance-matched exactly at the LC tuning state with maximum dielectric dissipation (i.e. nematic state with laser light-off), and least matched at the state with minimum dielectric dissipation (i.e. isotropic state), hence allowing a minimised variation in the total insertion loss across the full range of differential phase shift (i.e. 0 to 180°, controlled accordingly by the light intensity).

In addition, the transparent ITO is precisely modelled with adaptive meshing inside metals, instead of conventional surface impedance model without solving fields inside. Accordingly, the width of the microstrip is derived as 0.29 mm for the mainline, tapering to 0.64 mm for the connectors-to-substrate interfaces based on time-domain reflectometry to mitigate impedance mismatch due to higher-order modes at geometrical discontinuities. Targeting a phase shift capability up to 180° at 10 GHz, the total length of the core line is experimentally optimised to be 30.6 cm after iterations of prototypes.

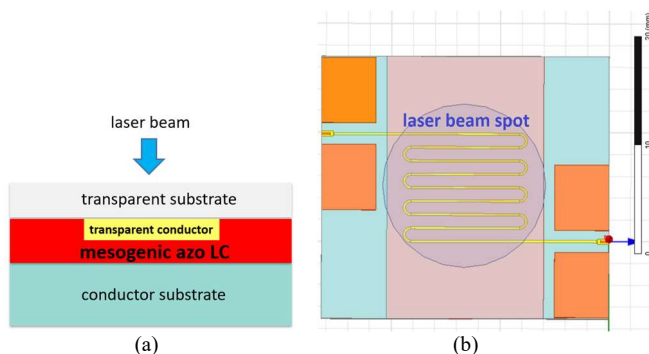


Fig. 1. Schematic of the phase shifter (a) cross-section view; (b) top view.

III. MEASUREMENT RESULTS AND DISCUSSION

The mesogenic azo LC mixture (10 wt% CPND-7 dissolved in GT3-24002) is characterised using 10 μm -thick cells. By polarising microscopy, the nematic phase in trans isomers is confirmed for the mixture at the laser light-off state. Using a spectrophotometer (JASCO), the unpolarised absorption spectra (Fig. 2) reports the absorption peak at 465 nm. Accordingly, a compact 465 nm blue laser (continuous-wave operation) with a beam expander in Fig. 3 (a) is adapted for a focus beam diameter of 3 cm to cover the effective transmission line area targeting a maximum of 180° phase shift at 10 GHz. Using an optical chopper and a photodiode power meter, response times of the 10 μm -thick cell are measured, reporting a switching-on time of 250 milliseconds (corresponding to the photochemically induced trans–cis transition) and a switching-off time of 700 milliseconds (corresponding to the thermal cis-trans back-isomerization). Free of undesirable storage effects, the mesogenic azo LC mixture is demonstrated practical for specific microwave beamforming applications with moderate or slow phase-shifting speed requirement, such as in radio telescopes for sky survey [17], and satellite relay links [5], i.e. low-earth orbit (LEO) satellites tracking from geosynchronous (GEO) satellites.

Based on the material properties measured, a phase shifter prototype is fabricated as shown in Fig. 3 (b), with connectors flange-mounted on the grounding plate for S-parameters testing using a two-port vector network analyser. Note that the device fabrication is based on our established LC-based device assembly process [18]–[23]. First, the designed meander delay line is patterned on an ITO-coated glass by photolithography and chemical etching. Alignment agent (polyimide AL1254) is spin-coated on the patterned glass and the grounding plane, then anti-parallelly rubbed by a roller to produce surface anchoring alignment for the mesogenic azo LC at the laser light-off state. The azo LC mixture is filled into the device cavity by capillary action, with the cavity's openings sealed by glue and UV-cured. For maximum optical absorption, the assembled device under test in Fig. 3 (b) is positioned at a normal incidence angle with the laser beam, whose polarisation is parallel with the rubbing direction.

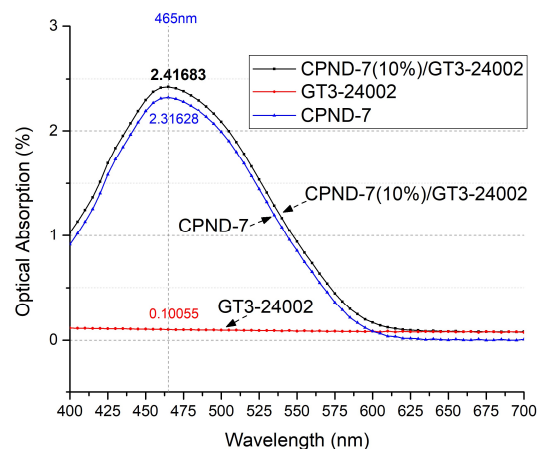


Fig. 2. Absorption spectra measured for GT3 LC mixed with CPND-7 azo dye.

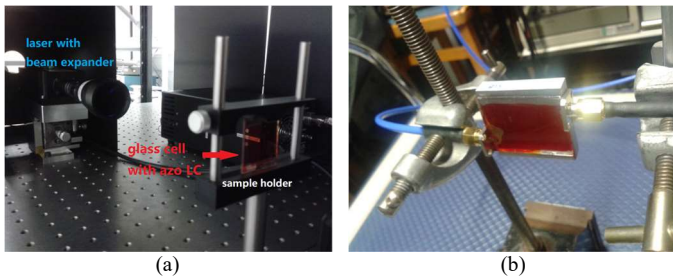


Fig. 3. Photographs of experimental setup and fabricated phase shifter: (a) laser with beam expander setup and power calibration; (b) assembled phase shifter measured with a vector network analyser (laser light-off state).

Modulating the laser supply current up to 3 A, the differential phase shift and insertion loss of the phase shifter over 1–10 GHz are obtained in Figs. 4 and 5. A maximum phase shift of 184° at 10 GHz is reported with an insertion loss of -3.53 dB (including connectors) and return loss up to -12 dB (for the least matched state evidenced by the phase shift-frequency ripples). Decreasing the laser current from 3 A progressively to 0 (i.e. light off), the differential phase shift dynamically drops from 184° to nearly 0° , demonstrating a reversible phase tuning with analog resolution. Furthermore, Fig. 5 proves that the variation of the insertion loss across the full range of phase shifts is negligible (agreed within statistics considering manufacturing tolerances) for each individual frequency, as further evidenced by a flattened profile in Fig. 6. The maximum variation in the measured insertion loss among different shifting states at 10 GHz is only up to 9% (with the fabrication tolerance), i.e. a significant reduction in the undesirable variation as compared with the state-of-the-art LC-based phase shifter [13] reported with 30%. These properties are highly useful for phased array analog beam steering targeting minimum beam distortions.

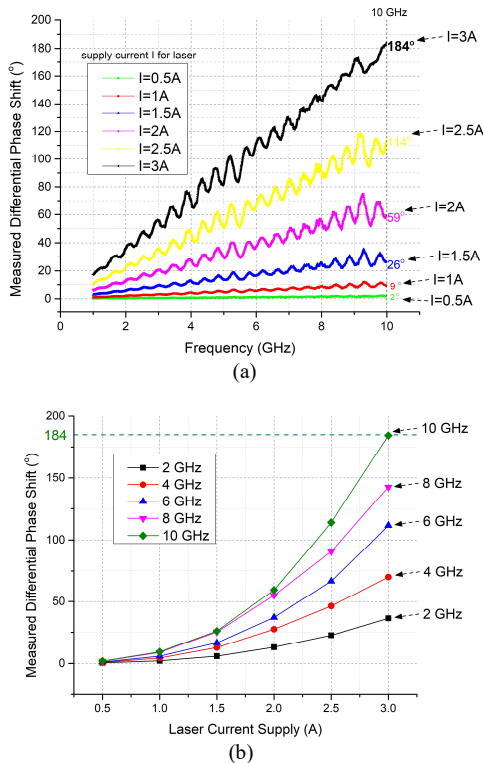


Fig. 4. Measured differential phase shift (a) vs. frequency; (b) vs. laser current.

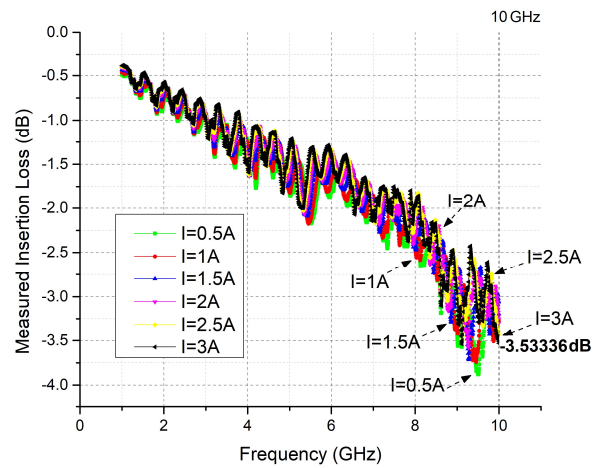


Fig. 5. Measured insertion loss at different modulation states.

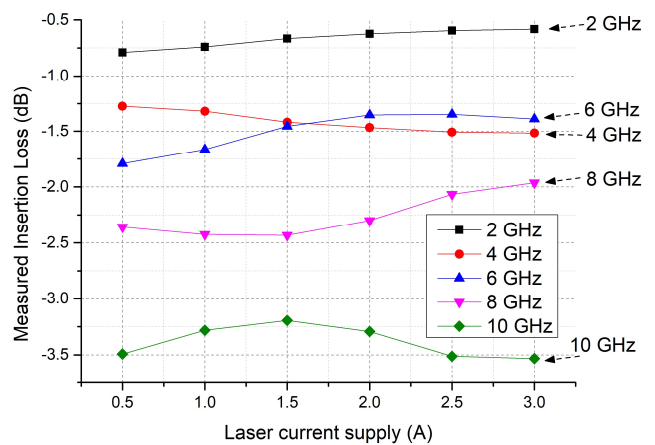


Fig. 6. Measured insertion loss under different laser supply currents (i.e. different phase-shifting states) for different frequencies.

For a more comprehensive evaluation of the phase shift and insertion loss performance, the figure-of-merit (FoM) is quantified in Fig. 7 based on the ratio of the maximum phase shift to the maximum insertion loss (max. IL). The optimum FoM in excess of $60^\circ/\text{dB}$ is obtained at 6 and 7 GHz, as distinct from the traditional monotonically increasing FoM from 1 to 10 GHz [13] up to $42^\circ/\text{dB}$. Table I below summarises our device performance compared against other state-of-the-art LC-based continuously tuned (analog) phase shifters at 10 GHz.

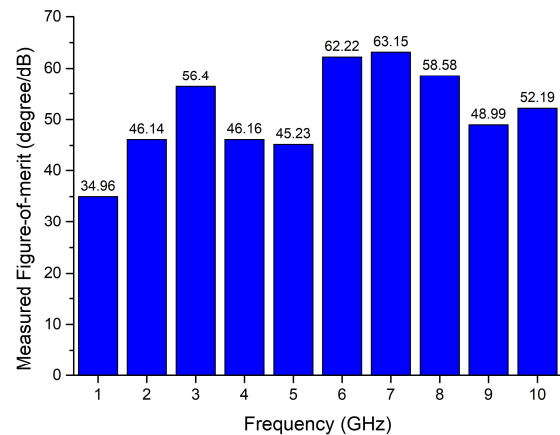


Fig. 7. Measured figure-of-merit of the phase shifter device from 1 to 10 GHz.

TABLE I
MEASURED PERFORMANCE COMPARED WITH STATE-OF-THE-ART LC-BASED
ANALOG PHASE SHIFTERS AT 10 GHz

Ref.	Bias networks	Phase shift (°)	max.IL (dB)	FoM (°/dB)	IL balancing
[7]	yes	150	-3.5	42.9	no
[10]	yes	125	-2.0	62.5	no
[11]	yes	50	-2.6	19.2	no
[12]	yes	100	-3.0	33.3	no
[13]	yes	360	-8.5	42.4	no
This work	free	184	-3.5	52.1	yes

As evidenced in Table I, this work exhibits unique advantages of bias network free and insertion loss balancing. The FoM of 52.1°/dB outperforms most of the up-to-date documentation [7][11]–[13] at 10 GHz, and remains highly comparable with [10] if the insertion loss of our device could be further reduced by optimising the thickness of the mesogenic azo LC, synthesizing the azo LC mixture with a lower dissipation factor at the target frequency range, and exploring a transparent conductor with a lower electrical sheet resistance.

In addition to these optimisation possibilities, the device configuration of our first prototype (Fig. 1) can be modified to address the lossy transparent conductor problem (mainly for the core line) at microwave frequencies. As shown in Fig. 8 below, the illumination of the laser beam can be arranged to pass through the ground plane (in a transparent conductor), while the meander core line can be a low-loss conductor (e.g. copper) without the requirement for optical transparency. In this way, the core line can be patterned on microwave low-loss dielectric laminates (e.g. supplied from Rogers or Taconic) using the well-established and low-cost printed circuit board manufacturing techniques. Therefore, the total conductor loss as well as the manufacturing tolerance could be further reduced for an even higher figure-of-merit.

Furthermore, the device miniaturisation towards millimetre-wave frequencies and the shifting range scalability towards 360° are promising with the beam expander eliminated, allowing a lower laser power supply for extended applications. Last but not least, the proposed optical driving allows segmented phase shift control of the delay line by moving the beam spot, adding another degree of reconfigurability for a phased array feeding system.

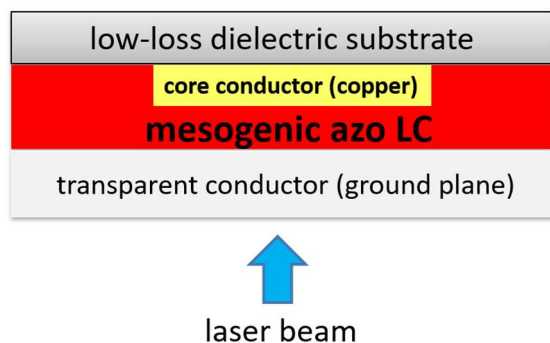


Fig. 8. A new device configuration proposed for future investigation of the insertion loss mitigation.

IV. CONCLUSION

An unconventional optically controlled microwave phase shifter realised by mesogenic azo LC mixture is designed, fabricated, and measured across 1–10 GHz. By modulating the intensity of a laser beam, the device exhibits an analog shifting capability from 0° to 184° with an insertion loss of –3.53 dB at 10 GHz. Free of phase biasing networks for the mesogenic azo LC, the standalone device solution is free from associated noises degrading the phase-shifting resolution. With insertion losses balanced in all phase-shifting states, the device is also free of amplitude compensation networks for integration into a phased array beam-steering system. The proposed true-time-delay all-optically addressed analog phase shifter with mitigated beam distortions is promising to expand and unlock a wide variety of forward-thinking scenarios targeting microwave beamforming applications, such as the future standalone mobile communication network [24][25], advanced in-core detector systems for static safety inspections [26] of a nuclear power plant without mechanical movements, as well as the Square Kilometre Array (SKA) radio telescopes [27] for studying the universe.

REFERENCES

- [1] I. Uchendu, and J. R. Kelly, “Survey of Beam Steering Techniques Available for Millimeter Wave Applications,” *Prog. Electromagn. Res. B*, vol. 68, pp. 35–54, 2016.
- [2] D. Parker, and D. C. Zimmermann, “Phased arrays - part 1: theory and architectures,” *IEEE Transactions on Microwave Theory and Techniques*, vol. 50, no. 3, pp. 678–687, March 2002.
- [3] P. Yaghmaee, O.H. Karabey, B. Bates, C. Fumeaux, and R. Jakoby, “Electrically Tuned Microwave Devices Using Liquid Crystal Technology,” *Int. J. Antenn. Propag.*, vol. 2013, 824214, 2013.
- [4] J. Li, H. Xu, and D. Chu, “Design of liquid crystal based coplanar waveguide tunable phase shifter with no floating electrodes for 60–90 GHz applications,” in 2016 46th European Microwave Conference (EuMC), London, 2016, pp. 1047–1050.
- [5] H. Maune, M. Jost, R. Reese, E. Polat, M. Nickel, and R. Jakoby, “Microwave Liquid Crystal Technology,” *Crystals*, vol. 8, 9, 355, 2018.
- [6] D. C. Zografopoulos, A. Ferraro, and R. Beccherelli, “Liquid-crystal high-frequency microwave technology: Materials and Characterization,” *Adv. Mater. Technol.*, vol. 4, 2, 1800447, December 2018.
- [7] O. H. Karabey, A. Gaebler, S. Strunck, and R. Jakoby, “A 2-D Electronically Steered Phased-Array Antenna With 2×2 Elements in LC Display Technology,” *IEEE Transactions on Microwave Theory and Techniques*, vol. 60, no. 5, pp. 1297–1306, May 2012.
- [8] O. H. Karabey, A. Mehmood, M. Ayluctarhan, H. Braun, M. Letz, and R. Jakoby, “Liquid crystal based phased array antenna with improved beam scanning capability,” *Electronics Letters*, vol. 50, no. 6, pp. 426–428, 13 March 2014.
- [9] L. Cai, H. Xu, J. Li, and D. Chu, “High FoM liquid crystal based microstrip phase shifter for phased array antennas,” in 2016 International Symposium on Antennas and Propagation (ISAP), Okinawa, 2016, pp. 402–403.
- [10] S. Muller, P. Scheele, C. Weil, M. Wittek, C. Hock, and R. Jakoby, “Tunable passive phase shifter for microwave applications using highly anisotropic liquid crystals,” in Proceedings of the IEEE MTT-S International Microwave Symposium Digest, Fort Worth, TX, USA, 6–11 June 2004; pp. 1153–1156.
- [11] S. Bulja, and D. M. Syahkal, “Meander line millimetre-wave liquid crystal based phase shifter,” *Electronics Letters*, vol. 46, no. 11, pp. 769–771, 27 May 2010.
- [12] J. Piotrowski, J. Parka, and E. N. Kruszelnicki, “Nematic liquid crystals in inverted microstrip structures,” *Proc. SPIE 8902*, Electron Technology Conference 2013, 89022B, 25 July 2013.

- [13] L. Cai, H. Xu, J. Li, and D. Chu, "High figure-of-merit compact phase shifters based on liquid crystal material for 1–10 GHz applications," *Jpn. J. Appl. Phys.*, vol. 56, 011701, November 2017.
- [14] U. Hrozhyk, S. Serak, N. Tabiryany, D. Steeves, L. Hoke, and B. Kimball: "Azobenzene liquid crystalline materials for efficient optical switching with pulsed and/or continuous wave laser beams," *Opt. Express*, vol. 18, 8, 2010, pp. 8697–8704.
- [15] L. Su, B. Wang, J. West, and Y. Reznikov, "Liquid crystal photoalignment on azo-dye layers," *Mol. Cryst. Liq. Cryst.*, vol. 359, 1, 2006, pp. 147–155.
- [16] U. Hrozhyk, S. Serak, N. Tabiryany, D. Steeves, L. Hoke, and B. Kimball, "Azobenzene liquid crystals for fast reversible optical switching and enhanced sensitivity for visible wavelengths," Proc. SPIE 7414, Liquid Crystals XIII, 74140L, California, United States, August 2009.
- [17] E. A. K. Adams, and J. V. Leeuwen, "Radio surveys now both deep and wide," *Nature Astronomy*, vol. 3, 188, February, 2019.
- [18] J. Li and D. Chu, "Liquid crystal-based enclosed coplanar waveguide phase shifter for 54–66 GHz applications," *Crystals*, vol. 9, 12, 650, December 2019.
- [19] A. Yontem, J. Li, and D. Chu, "Imaging through a projection screen using bi-stable switchable diffusive photon sieves," *Opt. Express*, vol. 26, pp. 10162–10170, April 2018.
- [20] J. Li, "Structure and Optimisation of Liquid Crystal based Phase Shifter for Millimetre-wave Applications," doctoral thesis, University of Cambridge, Cambridge, 2019.
- [21] J. Li, "Bias Tees Integrated Liquid Crystals Inverted Microstrip Phase Shifter for Phased Array Feeds," in 21st International Conference on Electronic Packaging Technology (ICEPT), Guangzhou, 2020.
- [22] J. Li, "Low-loss tunable dielectrics for millimeter-wave phase shifter: from material modelling to device prototyping," in IOP Conference Series: Materials Science and Engineering, 2020.
- [23] J. Li, "60 GHz Optimised Nickel-free Gold-plated Enclosed Coplanar Waveguide Liquid Crystal Phase Shifter," in International Microwave Workshop Series on Advanced Materials and Processes for RF and THz Applications (IEEE MTT-S IMWS-AMP), Suzhou, 2020.
- [24] S. I. Popoola, N. Faruk, A. A. Atayero, M. A. Oshin, O. W. Bello, and M. Adigun, "5G Radio Access Network Technologies: Research Advances," in Proceedings of the World Congress On Engineering and Computer Science, WCECS 2017, 2017, vol. I, pp. 101–105.
- [25] O. T. Eluwole, N. Udoh, M. Ojo, C. Okoro, and A. J. Akinyoade, "From 1G to 5G, what next?," *IAENG Int. J. Comput. Sci.*, vol. 45, no. 3, pp. 413–434, 2018.
- [26] J. Li, "Fault-Event Trees Based Probabilistic Safety Analysis of a Boiling Water Nuclear Reactor's Core Meltdown and Minor Damage Frequencies," *Safety*, vol. 6, 2, 28, June 2020.
- [27] P. E. Dewdney, P. J. Hall, R. T. Schilizzi, and T. J. Lazio, "The Square Kilometre Array," *Proc. IEEE*, vol. 97, no. 8, pp. 1482–1496, August 2009.